

Host Expression Profiling From Diagnostic Coronavirus Disease 2019 Swabs Associates Upper Respiratory Tract Immune Responses With Radiologic Lung Pathology and Clinical Severity

Robert A. Kozak,^{1,2,3} Elsa Salvant,¹ Veronica Chang,¹ Anastasia Oikonomou,¹ Mia J. Biondi,^{4,5} Jordan J. Feld,⁵ Susan Armstrong,¹ Sumaiyah Wasif,¹ Samira Mubareka,^{1,3} Kuganya Nirmalarajah,¹ Arun Seth,^{1,6} Yutaka Amemiya,¹ Chao Wang,^{1,7} and Hubert Tsui^{1,3,6,7}

¹Biological Sciences Platform, Sunnybrook Research Institute, Toronto, Ontario, Canada, ²Shared Hospital Laboratory, Toronto, Ontario, Canada, ³Department of Laboratory Medicine and Pathobiology, University of Toronto, Toronto, Ontario, Canada, ⁴School of Nursing, York University, Toronto, Ontario, Canada, ⁵Toronto Centre for Liver Disease, University Health Network, Toronto, Ontario, Canada, ⁶Precision Diagnostics and Therapeutics Program, Department of Laboratory Medicine and Molecular Diagnostics, Sunnybrook Health Sciences Centre, Toronto, Ontario, Canada, and ⁷Department of Immunology, University of Toronto, Toronto, Ontario, Canada

Background. COVID-19 presents with a breadth of symptomatology including a spectrum of clinical severity requiring intensive care unit (ICU) admission. We investigated the mucosal host gene response at the time of gold standard COVID-19 diagnosis using clinical surplus RNA from upper respiratory tract swabs.

Methods. Host response was evaluated by RNA-sequencing, and transcriptomic profiles of 44 unvaccinated patients including outpatients and in-patients with varying levels of oxygen supplementation were included. Additionally, chest X-rays were reviewed and scored for patients in each group.

Results. Host transcriptomics revealed significant changes in the immune and inflammatory response. Patients destined for the ICU were distinguished by the significant upregulation of immune response pathways and inflammatory chemokines, including *cxcl2* which has been linked to monocyte subsets associated with COVID-19 related lung damage. In order to temporally associate gene expression profiles in the upper respiratory tract at diagnosis of COVID-19 with lower respiratory tract sequelae, we correlated our findings with chest radiography scoring, showing nasopharyngeal or mid-turbinate sampling can be a relevant surrogate for downstream COVID-19 pneumonia/ICU severity.

Conclusions. This study demonstrates the potential and relevance for ongoing study of the mucosal site of infection of SARS-CoV-2 using a single sampling that remains standard of care in hospital settings. We highlight also the archival value of high quality clinical surplus specimens, especially with rapidly evolving COVID-19 variants and changing public health/vaccination measures.

Keywords. COVID-19; diagnostic swab; host-response; lower respiratory tract infection; RNA sequencing.

Infection with severe acute respiratory syndrome coronavirus 2 (SARS-CoV-2) can result in a spectrum of disease severity that ranges from asymptomatic to intensive care unit (ICU)-level support and fatality. The difference in outcomes is multifactorial and related to intrinsic patient variables such as age and comorbidities as well as variations in viral-host immune responses [1–4], for example, alterations in interferon (IFN) signaling [5] and

high serum levels of proinflammatory cytokines such as interleukin 6 and tumor necrosis factor- α [6]. Gene expression studies examining the systemic response using peripheral blood mononuclear cells (PBMCs) have associated persistent viremia and dysregulated inflammation, combined with low or nonexistent levels of type I IFNs, to patients with severe disease [7]. While circulating mononuclear cells may provide valuable information, the translational potential of cellular immunity assays to the clinical laboratory is limited by practical barriers related to processing of live cells and the complexity and time-consuming nature of such assays. Study of systemic blood-derived immune responses may also differ from important local effects directly at the likely initiating site of viral exposure.

Recent work examining multiple datasets from the nasal specimens and pulmonary tissues of patients with coronavirus disease 2019 (COVID-19) identified a relationship between disease severity and 14 type I IFN-inducible genes [8]. In contrast, spatial transcriptomic analysis of lung tissue from patients with fatal COVID-19 pneumonitis found common IFN- γ expression

Received 11 January 2023; editorial decision 31 March 2023; accepted 11 April 2023; published online 13 April 2023

Correspondence: Hubert Tsui, MD, PhD, FRCPC, Sunnybrook Research Institute, 2075 Bayview Ave, Toronto, ON M4N 3M5, Canada (hubert.tsui@sunnybrook.ca); Robert A. Kozak, PhD, FCCM, Sunnybrook Research Institute, 2075 Bayview Ave, Toronto, ON M4N 3M5, Canada (rob.kozak@sunnybrook.ca).

Open Forum Infectious Diseases®

© The Author(s) 2023. Published by Oxford University Press on behalf of Infectious Diseases Society of America. This is an Open Access article distributed under the terms of the Creative Commons Attribution-NonCommercial-NoDerivs licence (<https://creativecommons.org/licenses/by-nc-nd/4.0/>), which permits non-commercial reproduction and distribution of the work, in any medium, provided the original work is not altered or transformed in any way, and that the work is properly cited. For commercial re-use, please contact journals.permissions@oup.com

<https://doi.org/10.1093/ofid/ofad190>

(a type II IFN) by local cytotoxic lymphocytes and induced chemokine patterns in the most severely damaged tissue areas [9]. The diversity and importance of IFN signaling relative to the anatomic site is further highlighted by the divergent/dynamic expression of type III IFN genes in certain parts of the respiratory tract [10]. Indeed, RNA sequencing (RNAseq) of research nasopharyngeal (NP) swabs from patients in the United States noted enrichment of IFN pathway-associated genes, chemokine patterns such as CXCL10, CXCL11, and CCL8 genes linked to higher viral burdens of SARS-CoV-2 [11]. However, as with many studies, the comparator was to healthy or non-SARS-CoV-2-infected patients and not directly addressing the spectrum of disease severity. Nonetheless, differences in upper respiratory host gene expression may be a valuable predictor between an immune response supporting viral clearance and an aberrant chronic inflammation that results in lower respiratory tract pathology [2]. This is an important clinical consideration that may be leveraged to guide healthcare resource utilization.

Here, we probed the utility of clinical surplus RNA derived from NP swabs used for initial detection of SARS-CoV-2 infection as an informative snapshot of the upper respiratory tract host environment that importantly coincides temporally with the initial real-world interface between patient and the healthcare system. By associating *in situ* host transcriptional and immunological response in the upper respiratory tract with clinical severity as gauged by supplementary oxygen requirements as well as lower respiratory sequelae using a radiographic scoring system from standard-of-care chest radiographs (CXRs), we highlight gene enrichment signatures that distinguished outpatient COVID-19-infected patients from patients with impending ICU admission. These data support the potential novel applicability of clinical upper respiratory tract sampling to predict severe lower respiratory sequelae.

METHODS

Patient Cohort

Unvaccinated COVID-19 patients were identified following a data query from the laboratory information system and required a positive reverse-transcription polymerase chain reaction (RT-PCR) test for inclusion in this study or were recruited as part of an interventional clinical trial, and the period of inclusion was from March 2020 to September 2020. A retrospective chart review was performed to obtain demographic data, and all patients were confirmed to have had no previously documented SARS-CoV-2 infection. Patients were categorized into the following groups based on previous studies [12, 13]: Group A included nonadmitted patients with no bloodwork performed; group B included nonadmitted patients with bloodwork performed; group C included admitted patients who did not require supplemental oxygen; group D

included admitted patients who required supplemental oxygen but not mechanical ventilation; and group E included admitted patients who required mechanical ventilation at any point during admission. No patients were transferred between groups or were reclassified. The retrospective chart review was approved by the Sunnybrook Health Sciences Centre Research Ethics Board (REB #1911), and the clinical trial was approved by all research ethics boards of all participating institutions, registered on ClinicalTrials.gov (NCT04354259), and conducted under a Clinical Trial Application approved by Health Canada.

RNA Extraction, Quantification, and Quality

Midturbinate (MT) or NP swabs were collected as part of routine diagnostics. Total nucleic acid extraction was performed using the NucliSENS EasyMAG (bioMérieux, France), and detection of SARS-CoV-2 RNA was performed using established clinical assays [14]; residual RNA was subsequently stored at -80°C for downstream analysis. The total nucleic acid was separated on a 2100 Bioanalyzer system using the RNA 6000 Pico Kit (Agilent, Santa Clara, California) for sample quality assessment. The amount of amplifiable human origin total RNA was estimated by amplifying exons spanning the 96 bp coding region in the human β -glucuronidase gene (GUSB). The qPCR reaction was carried out in 10 μL with 1 \times TaqMan Fast Virus Mix, 1 \times Human GUSB assay mix (Hs0093962_m1, ThermoFisher Scientific, Waltham, Massachusetts), and 2 μL of extracted total RNA by using the StepOnePlus Real-Time PCR System (ThermoFisher Scientific). The PCR cycling conditions were 50°C for 5 minutes, 95°C for 20 seconds, 40 cycles of 95°C for 3 seconds, and 60°C for 1 minute. Standard curves for total RNA quantification were prepared using HL-60 Total RNA (ThermoFisher Scientific).

Targeted Transcriptome Sequencing

To determine whether the host transcriptome coinciding with the real-world sampling time of clinical COVID-19 diagnosis shows a distinct pattern associated with disease severity, we sequenced residual material from clinical MT/NP swabs using the Ion Torrent platform comprising a single multiplexed panel targeting 18 574 coding and 2228 non-coding RefSeq genes (>95% of the RefSeq gene database).

The targeted human transcriptome sequencing was performed on the Ion S5XL Next Generation Sequencing system with the Ion AmpliSeq Transcriptome Human Gene Expression Panel (ThermoFisher Scientific). Fifty picograms to 1 ng of total RNA quantified by GUSB qPCR assay was treated with ezDNase for removal of genomic DNA contamination in the sample and then reverse-transcribed in a 15- μL reaction using the SuperScript IV VILO Master Mix with ezDNase Enzyme kit. The barcoded complementary DNA libraries were constructed by using Ion AmpliSeq Transcriptome

Human Gene Expression Panel, Chef-Ready Kit. The targeted sequences were PCR amplified for 18 cycles with a 16-minute extension time. Quantification of the libraries was done using the Ion Library TaqMan Quantitation Kit (ThermoFisher Scientific). The final library concentration was diluted to 60 pM. The sequencing template preparation was done using Ion Chef with Ion 550 Chef Kits. Sequencing was performed for 500 flows on an Ion S5XL Sequencer with Ion 550 chip.

Data Analysis

The Ion Torrent platform-specific pipeline software Torrent Suite version 5.16.0 (ThermoFisher Scientific) was used to separate barcoded reads and to filter and remove polyclonal and low-quality reads. The sequencing data were aligned and mapped to the panel-specific reference sequence file (hg19_amplicon_transcriptome_ercc_v1) using the Ion Torrent Mapping Alignment Program, which is optimized for Ion Torrent data. Data were subsequently normalized, and differential gene expression was analyzed using EdgeR and Limma [15, 16]. Benjamini-Hochberg (BH) adjusted *P* value of <.05 is reported. Pathway analysis was performed using Gene Set Enrichment Analysis and MSigDB (<https://www.gsea-msigdb.org/gsea/index.jsp>) and Reactome (www.reactome.org).

Analysis of Radiographic Findings

The CXRs were reviewed and scored by a radiologist who was blinded to the patient group using a modified CXR score for COVID-19 infection combining extent of the disease and density of the lesions [17, 18]. In total, 18 images were available for review for the entire cohort. For each patient, the CXR with the most severe findings—that was taken within 10 days of diagnosis—was collected.

RESULTS

Cohort Description

Our cohort included a total of 38 individuals, of whom 68.4% were admitted and 31.6% nonadmitted patients. The mean age was 60.9 years (range, 23–95 years) and 39% (*n* = 15) were male. The average number of days from symptom onset to a positive COVID-19 test in group A was 4.71 (*n* = 12), in group C was 4.99 (*n* = 10), in group D was 1.57 (*n* = 9), and in group E was 6.5 (*n* = 8). Admitted patients had more comorbidities than nonadmitted patients. Only 3 patients were on immunosuppressants, and no one in the cohort had documented infection with human immunodeficiency virus. The percentages of comorbidities are included in Supplementary Table 1. No patients from group B were identified. Four patients died within 30 days of diagnosis; 2 were part of group C and 2 were part of group E, and they had been admitted to the ICU.

Distinct Gene Patterns Associated With Disease Severity

Overall, our RNAseq and subsequent gene expression analyses identified a total of 184 differentially expressed genes (DEGs; BH adjusted *P* < .05) across the cohort (Figure 1). Focusing on the cohort of nonadmitted COVID-19 patients (group A) compared to COVID-19 patients who required ICU admission after the initial sampling time (group E), we identified 59 DEGs between these 2 groups (Figure 1A and 1B and Supplementary Table 1). Notable changes included chemokine genes *cxcl2* and *cxcl3*, which were both upregulated in the ICU (group E) cohort and known to recruit a monocyte/neutrophil-dominant infiltrate. Interestingly, these chemokines may signify the presence of a highly proinflammatory COVID-19-associated monocyte subset, designated as Mono_c1-CD14-CCL3, as characterized from single cell analyses of PBMCs and bronchoalveolar lavage (BAL) fluids [19]. Additional genes of interest include *MYC* and *EGR1*, which were also upregulated in the ICU cohort. These are 2 targets of inflammasome activation, consistent with recent work showing activation of inflammasome in macrophages driving COVID-19 pathology [20]. In contrast, nonadmitted patients (group A) have increased expression of genes involved in processes such as antigen processing (*clec2D*), circadian clock (*Per3*), and nonsense-mediated messenger RNA decay (*SMG6*), which protects cells from gene expression errors. These findings indicate in situ differences in the upper respiratory tract at the time of clinical presentation to hospital and diagnosis of COVID-19, suggesting that biomarkers related to an activated monocytic inflammatory microenvironment may be of use to stratify COVID-19 patients at risk for a more severe disease trajectory, typically involving the lower respiratory tract. Note that the differences between group A and group E are not explained by SARS-CoV-2 viral load (data not shown), consistent with other reports [21].

Transcriptional Profiles Within Hospitalized Patients

Different gene expression patterns across admitted patients were also compared. Between patients with ICU admission (group E) and inpatients without need for supplemental oxygen (group C), 124 DEGs were identified with a particularly strong signal in *HMGCS1*. Upregulation of this gene is also seen when comparing the ICU cohort with nonadmitted patients (Figure 1C). Interestingly, *HMGCS1* encodes the mevalonate precursor enzyme, 3-hydroxy-3-methylglutaryl-CoA synthase 1, which catalyzes the conversion of cytosolic acetoacetyl-CoA to 3-hydroxy-3-methylglutaryl-CoA, a necessary step in mevalonate synthesis [22]. Involvement of this pathway is postulated to reflect hijacked cholesterol metabolism that may be necessary for SARS-CoV-2 replication [23]; however, given the general lack of association of between viral load and clinical severity, whether *HMGCS1* is a marker of increased stem cell activation in response to damage may be another explanation. Additionally, the *SUMO2* and *SPR* genes, both involved in

Table 1. Top Dysregulated Host Pathways in Intensive Care Unit Patients Compared to Hospitalized Patients

Pathway Name	Entities Found	Ratio	P Value	FDR	Reactions Found	Ratio
ROBO receptors bind AKAP5	3/11	7.22×10^{-4}	1.43×10^{-4}	0.093	4/7	4.95×10^{-4}
RET signaling	4/43	3.00×10^{-3}	6.42×10^{-4}	0.1	3/24	0.002
SUMOylation of transcription cofactors	4/44	0.003	6.99×10^{-4}	0.1	6/27	0.002
Activated NTRK3 signals through PLCG1	2/5	3.28×10^{-4}	9.60×10^{-4}	0.1	3/3	2.12×10^{-4}
SUMOylation of DNA replication proteins	4/50	0.003	1.00×10^{-3}	0.1	3/8	5.65×10^{-4}
SUMOylation of RNA binding proteins	4/51	3.00×10^{-3}	1.00×10^{-3}	0.1	3/4	2.83×10^{-4}
Inositol phosphate metabolism	5/90	6.00×10^{-3}	1.00×10^{-3}	0.1	10/71	0.005
SUMO E3 ligases SUMOylate target proteins	7/183	1.20×10^{-2}	1.00×10^{-3}	0.1	47/131	0.009
DAG and IP3 signaling	4/53	0.003	1.00×10^{-3}	0.1	7/28	0.002
SUMOylation	7/192	0.013	2.00×10^{-3}	0.1	52/140	0.01
SUMO is transferred from E1 to E2 (UBE2I, UBC9)	2/7	4.59×10^{-4}	2.00×10^{-3}	0.1	2/3	2.12×10^{-4}
PKA-mediated phosphorylation of key metabolic factors	2/7	4.59×10^{-4}	2.00×10^{-3}	0.1	3/5	3.53×10^{-4}
SUMO is conjugated to E1 (UBA2:SAE1)	2/8	5.25×10^{-4}	2.00×10^{-3}	0.112	2/3	2.12×10^{-4}
SUMOylation of chromatin organization proteins	4/62	0.004	2.00×10^{-3}	0.112	6/15	0.001
Synthesis of IP2, IP, and Ins in the cytosol	3/32	2.00×10^{-3}	3.00×10^{-3}	0.133	6/14	9.89×10^{-4}
Nucleotide excision repair	5/119	8.00×10^{-3}	4.00×10^{-3}	0.16	20/37	0.003
HuR (ELAVL1) binds and stabilizes mRNA	2/12	7.87×10^{-4}	5.00×10^{-3}	0.16	3/7	4.95×10^{-4}
SUMOylation of SUMOylation proteins	3/39	0.003	5.00×10^{-3}	0.16	2/5	3.53×10^{-4}
Processing of capped intron containing pre-mRNA	8/299	0.02	6.00×10^{-3}	0.16	32/34	0.02
Processing and activation of SUMO	2/13	8.53×10^{-4}	6.00×10^{-3}	0.16	5/9	6.36×10^{-4}
SUMOylation of DNA damage response and repair proteins	4/81	5.00×10^{-3}	6.00×10^{-3}	0.16	12/24	0.02
Transcriptional regulation by small RNAs	4/81	0.005	6.00×10^{-3}	0.16	2/5	3.53×10^{-4}
Triglyceride catabolism	3/42	0.003	7.00×10^{-3}	0.16	3/17	0.01

This table was generated using Reactome.

Abbreviations: FDR, false discovery rate; mRNA, messenger RNA.

inflammation, were also dysregulated. Interestingly, SUMO2 levels have been shown to be increased by SARS-CoV-2 infection of cells and result in increased Nf-KB activation and proinflammatory cytokine expression [24].

Alteration of Host Pathways and Subsequent Lower Respiratory Tract Involvement

We next performed an in silico analysis for enriched specific host response pathways using Gene Set Enrichment Analysis and MSigDB and Reactome. The pathways identified are shown in Table 1. The top identified pathways in the admitted but non-ICU (group C) versus ICU (group E) were associated with SUMOylation, which can lead to production of proinflammatory mediators. This suggested that dysregulation may result in inflammation and lower respiratory tract involvement. The acute clinical severity of COVID-19 infection and consequent need for ICU admission is primarily driven by lower respiratory tract infection/inflammation. To help address the adequacy of upper respiratory specimens for the diagnosis of clinically and radiographically significant lower respiratory tract disease or COVID-19 pneumonia, we asked whether standard-of-care MT/NP swab transcriptional profiles obtained at diagnosis temporally correlated with diagnostic lung imaging, the latter providing a noninvasive surrogate of lower respiratory tract progression. Blinded radiologists reviewed conventional CXRs for the cohort and were scored using accepted criteria

[17] (total score, sum of all lung quadrants). As shown in Figure 2, significant differences between ambulatory (group A) patients versus hospitalized, ICU-destined patients were found. Patients with the most severe disease (group E) also differed from admitted patients who did not require supplemental oxygen (group C). From a kinetic standpoint, these findings therefore solidify our upper respiratory tract (MT/NP swab)-derived transcriptomic findings at diagnosis of COVID-19 with clinically significant disease involving the lower respiratory tract.

DISCUSSION

The induction of cytokines, chemokines, and IFNs as part of the host response to SARS-CoV-2 infection is critical to determining disease severity, and multiple studies have associated inflammation with poor outcome in SARS-CoV-2 infection [2, 6, 7, 13, 25]. Analysis of gene signatures collected from the diagnostic swab would reflect the earliest localized immune response at the mucosal site of infection, which may differ from the systemic (ie, blood based) immune response. In this study, we used RNAseq to identify transcriptomic profiles among different clinically stratified patient groups, which were further supported by radiological findings.

Our data identified multiple DEGs between ambulatory (group A) and ICU (group E) patients, notably the chemokine

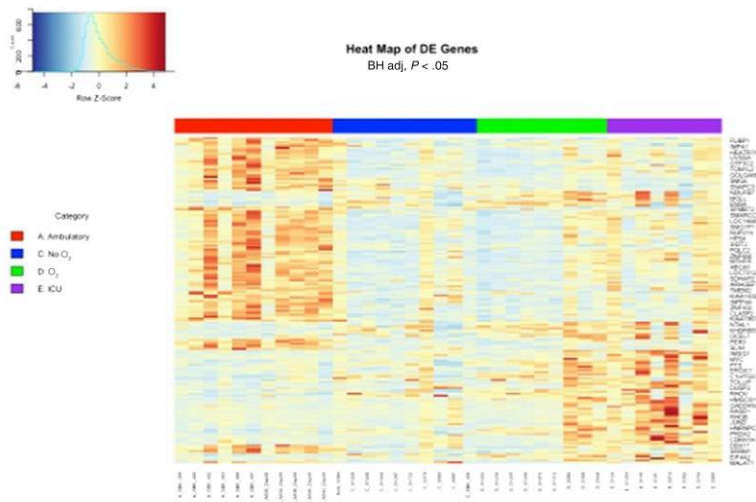
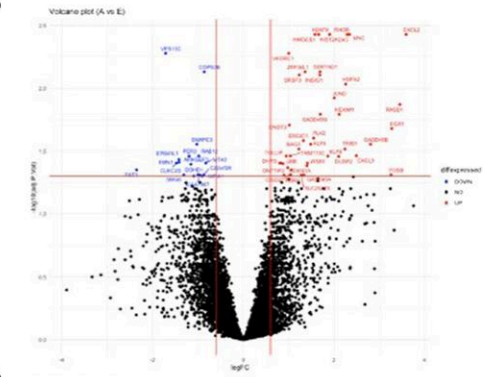
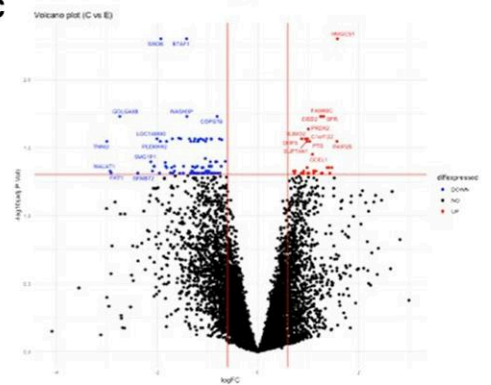
A**B****C**

Figure 1. Differentially expressed genes (DEGs) in patients with varying coronavirus disease 2019 disease severity. *A*, Heatmap of DEGs in each group ($P < .05$). *B* and *C*, Volcano plot for significant dysregulated genes in nonadmitted versus admitted patients (*B*) and in nonadmitted versus intensive care unit patients (*C*). Abbreviations: BH, Benjamini-Hochberg; DE, differentially expressed; ICU, intensive care unit; O₂, oxygen.

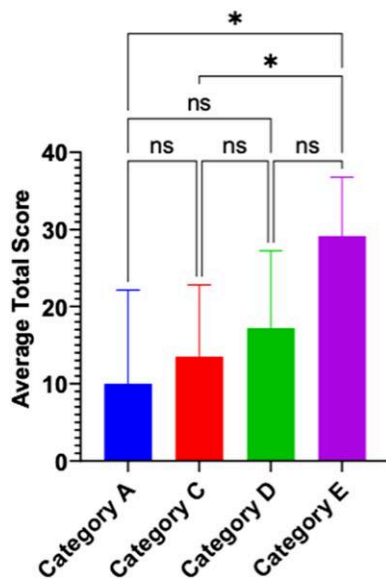


Figure 2. Average scores from chest radiographs from each group. The most severe image from each patient in group A ($n = 2$), group C ($n = 6$), group D ($n = 5$), and group E ($n = 6$) was analyzed and scored. Error bars represent standard deviation. $*P < .05$; ns, not significant.

genes *cxcl2* and *cxcl3*. This is consistent with a smaller study comparing the immune response in patients with moderate and severe COVID-19, which identified higher expression of *cxcl3* in moderate cases compared with healthy controls [25]. Interestingly, in our study, the expression of chemokine genes was associated with subsequent ICU admission and severe lung inflammation, the latter as evidenced by radiological findings during the initial 10 days after COVID-19 diagnosis. This temporal finding at clinical diagnosis of COVID-19 cannot be explained by duration of symptoms or viral load and suggests that a pre-SARS-CoV-2 exposure or intrinsic perturbed mucosal immune state may be contributing to a *cxcl1/cxcl3* biased immune response at risk for lower lung damage [9]. MYC and EGR1, 2 targets of inflammasome activation, were upregulated in the ICU cohort, consistent with recent work showing that activation of inflammasome in macrophages drives COVID-19 pathology [20]. Furthermore, EGR1 has been implicated in other highly pathogenic coronaviruses, notably severe acute respiratory syndrome coronavirus, and may serve a proviral role as it upregulates TGF- β 1 and a profibrotic response [26]. *HMGCS1* was also upregulated in the ICU cohort. This gene, which is part of the cholesterol biosynthesis pathway, was

recently identified as part of a genetic screen for factors important for coronaviral entry [27]. Thus, upregulation of *HMGCS1* may contribute to viral dissemination, resulting in inflammation and disease severity, and may partially explain the observed lung scores in our ICU patients. As the *HMGCS1* axis is also implicated in “stemness” properties related to cancer stem cells, one may also postulate whether this biomarker reflects a level of epithelial damage and initiation of regeneration programs [22, 28].

Our study had several limitations, notably that the cohort was relatively small after the necessary curation of high-quality RNA from clinically derived MT/NP swabs initially used solely for COVID-19 diagnostic RT-PCR. Furthermore, for patients in our nonadmitted group, we cannot rule out the possibility that they sought care and were admitted to other healthcare institutions, although this appears unlikely given the relatively homogeneous transcriptomic findings. Additionally, we used bulk RNAseq compared to single cell sequencing, the latter requiring a different biospecimen than the clinically archived material available in many laboratories at the start of the pandemic. Using single cell approaches, it has been highlighted that chemokine expression by monocytes/macrophages likely recruits cytotoxic lymphocytes that result in lung damage [9], including the BAL-defined mono_c1-CD14-CCL3 subset [19], which expresses abundant *cxcl2*. As single cell genomic resolution is impractical for most clinical applications, our concordant finding of *cxcl2* signals from bulk clinical upper respiratory tract swabs suggests this may be a biomarker worthy of further exploration.

CONCLUSIONS

Clinical surplus upper respiratory tract swab-derived RNA was used to evaluate its utility in probing host response at the time of real-world COVID-19 diagnosis. Significantly different transcriptomic profiles were found according to clinical severity. As part of routine care in hospital settings, our findings support the regimented archival of this material for research and future test development given its value as an *in situ* biomarker source for mucosal host-microbial interactions and link to lower respiratory tract progression. As reported with other viruses [29, 30], as well as SARS-CoV-2 [31], both host transcriptomic sequences and viral sequences can be captured from the same sample, allowing for simultaneous characterization of the pathogen [11]. This may support future companion diagnostics that characterize both viral and host genomic information to support clinical management as well as novel mucosal immune states as predisposing risk factors for adverse respiratory complications after infectious challenge.

Supplementary Data

Supplementary materials are available at *Open Forum Infectious Diseases* online. Consisting of data provided by the authors to benefit the reader, the posted materials are not copyedited and are the sole responsibility of

the authors, so questions or comments should be addressed to the corresponding author.

Notes

Author contributions. Conceptualization and study design: R. K., H. T. Experiments and investigation: E. S., S. A., S. W., Y. A., M. J. B., J. J. F., A. O., S. M., K. N. Analysis and summary of data: R. K., H. T., V. C., A. O., A. S., C. W., S. W., E. S., Y. A., S. A. Funding acquisition and supervision: R. K., H. T. Writing—original draft: R. K., M. J. B., H. T. All authors contributed thoughtful suggestions and resources, reviewed the manuscript, and approved the final version to be published. All authors agreed to be accountable for all aspects of the work.

Acknowledgments. We thank the volunteers who participated in this study; the Toronto Invasive Bacterial Disease Network; and all clinical, laboratory, and administrative teams who were involved in this work.

Financial support. This work was funded by the Canadian Institutes of Health Research (grant number OV5-170347 to R. K.); the Physician Services Incorporation Foundation (grant number 2020-1750 to H. T.); the Sunnybrook Health Sciences Centre Department of Laboratory Medicine and Molecular Diagnostics Strategic Innovation Fund (to H. T. and R. K.); and the Sunnybrook Health Sciences Centre Foundation (to R. K.).

Potential conflicts of interest. All authors: No reported conflicts.

References

1. Dos Santos JMB, Soares CP, Monteiro FR, et al. In nasal mucosal secretions, distinct IFN and IgA responses are found in severe and mild SARS-CoV-2 infection. *Front Immunol* **2021**; 12:595343.
2. Diamond MS, Kanneganti TD. Innate immunity: the first line of defense against SARS-CoV-2. *Nat Immunol* **2022**; 23:165–76.
3. Esai Selvan M. Risk factors for death from COVID-19. *Nat Rev Immunol* **2020**; 20:407.
4. Cillo AR, Somasundaram A, Shan F, et al. People critically ill with COVID-19 exhibit peripheral immune profiles predictive of mortality and reflective of SARS-CoV-2 lung viral burden. *Cell Rep Med* **2021**; 2:100476.
5. Bastard P, Rosen LB, Zhang Q, et al. Autoantibodies against type I IFNs in patients with life-threatening COVID-19. *Science* **2020**; 370:eabd4585.
6. Del Valle DM, Kim-Schulze S, Huang HH, et al. An inflammatory cytokine signature predicts COVID-19 severity and survival. *Nat Med* **2020**; 26:1636–43.
7. Hadjadj J, Yatim N, Barnabei L, et al. Impaired type I interferon activity and inflammatory responses in severe COVID-19 patients. *Science* **2020**; 369:718–24.
8. Zhang C, Feng YG, Tam C, Wang N, Feng Y. Transcriptional profiling and machine learning unveil a concordant biosignature of type I interferon-inducible host response across nasal swab and pulmonary tissue for COVID-19 diagnosis. *Front Immunol* **2021**; 12:733171.
9. Cross AR, de Andrea CE, Villalba-Esparza M, et al. Spatial transcriptomic characterization of COVID-19 pneumonitis identifies immune circuits related to tissue injury. *JCI Insight* **2023**; 8:e157837.
10. Sposito B, Broggi A, Pandolfi L, et al. The interferon landscape along the respiratory tract impacts the severity of COVID-19. *Cell* **2021**; 184:4953–68.e16.
11. Butler D, Mozsary C, Meydan C, et al. Shotgun transcriptome, spatial omics, and isothermal profiling of SARS-CoV-2 infection reveals unique host responses, viral diversification, and drug interactions. *Nat Commun* **2021**; 12:1660.
12. Kozak R, Armstrong SM, Salvant E, et al. Recognition of long-COVID-19 patients in a Canadian tertiary hospital setting: a retrospective analysis of their clinical and laboratory characteristics. *Pathogens* **2021**; 10:1246.
13. Bergamaschi L, Mescia F, Turner L, et al. Longitudinal analysis reveals that delayed bystander CD8+ T cell activation and early immune pathology distinguish severe COVID-19 from mild disease. *Immunity* **2021**; 54:1257–75.e8.
14. Kandel C, Zheng J, McCready J, et al. Detection of SARS-CoV-2 from saliva as compared to nasopharyngeal swabs in outpatients. *Viruses* **2020**; 12:1314.
15. Ritchie ME, Phipson B, Wu D, et al. Limma powers differential expression analyses for RNA-sequencing and microarray studies. *Nucleic Acids Res* **2015**; 43:e47.
16. Robinson MD, McCarthy DJ, Smyth GK. Edger: a bioconductor package for differential expression analysis of digital gene expression data. *Bioinformatics* **2010**; 26:139–40.
17. Murphy K, Smits H, Knoops AJG, et al. COVID-19 on chest radiographs: a multi-reader evaluation of an artificial intelligence system. *Radiology* **2020**; 296: E166–72.

18. Balbi M, Caroli A, Corsi A, et al. Chest X-ray for predicting mortality and the need for ventilatory support in COVID-19 patients presenting to the emergency department. *Eur Radiol* **2021**; 31:1999–2012.
19. Ren X, Wen W, Fan X, et al. COVID-19 immune features revealed by a large-scale single-cell transcriptome atlas. *Cell* **2021**; 184:1895–913.e19.
20. Sefik E, Qu R, Junqueira C, et al. Inflammasome activation in infected macrophages drives COVID-19 pathology. *Nature* **2022**; 606:585–93.
21. Jones TC, Biele G, Mühlemann B, et al. Estimating infectiousness throughout SARS-CoV-2 infection course. *Science* **2021**; 373:eabi5273.
22. Walsh CA, Akrap N, Garre E, et al. The mevalonate precursor enzyme HMGCS1 is a novel marker and key mediator of cancer stem cell enrichment in luminal and basal models of breast cancer. *PLoS One* **2020**; 15:e0236187.
23. Ziegler CGK, Miao VN, Owings AH, et al. Impaired local intrinsic immunity to SARS-CoV-2 infection in severe COVID-19. *Cell* **2021**; 184:4713–33.e22.
24. Li W, Qiao J, You Q, et al. SARS-CoV-2 Nsp5 activates NF-kappaB pathway by upregulating SUMOylation of MAVS. *Front Immunol* **2021**; 12:750969.
25. Chua RL, Lukassen S, Trump S, et al. COVID-19 severity correlates with airway epithelium-immune cell interactions identified by single-cell analysis. *Nat Biotechnol* **2020**; 38:970–9.
26. Li SW, Wang CY, Jou YJ, et al. SARS coronavirus papain-like protease induces Egr-1-dependent up-regulation of TGF-beta1 via ROS/p38 MAPK/STAT3 pathway. *Sci Rep* **2016**; 6:25754.
27. Wang R, Simoneau CR, Kulsuptrakul J, et al. Genetic screens identify host factors for SARS-CoV-2 and common cold coronaviruses. *Cell* **2021**; 184:106–19.e14.
28. Chen Y, Li M, Yang Y, Lu Y, Li X. Antidiabetic drug metformin suppresses tumorigenesis through inhibition of mevalonate pathway enzyme HMGCS1. *J Biol Chem* **2022**; 298:102678.
29. Yahya M, Rulli M, Toivonen L, Waris M, Peltola V. Detection of host response to viral respiratory infection by measurement of messenger RNA for MxA, TRIM21, and viperin in nasal swabs. *J Infect Dis* **2017**; 216:1099–103.
30. Kozak RA, Fraser RS, Biondi MJ, et al. Dual RNA-Seq characterization of host and pathogen gene expression in liver cells infected with Crimean-Congo hemorrhagic fever virus. *PLoS Negl Trop Dis* **2020**; 14:e0008105.
31. Islam ABMMK, Khan MA, Ahmed R, et al. Transcriptome of nasopharyngeal samples from COVID-19 patients and a comparative analysis with other SARS-CoV-2 infection models reveal disparate host responses against SARS-CoV-2. *J Transl Med* **2021**; 19:32.